Publisher source acknowledgment: https://doi.org/10.1002/cmdc.202000692

Synthesis and evaluation of voltage-gated sodium channel blocking pyrroline derivatives endowed with both antiarrhythmic and antioxidant activities

Alessia Carocci,*[a] Mariagrazia Roselli,[a] Roberta Budriesi,[b] Matteo Micucci,[b] Jean-François Desaphy,[c] Concetta Altamura,[c] Maria Maddalena Cavalluzzi,[a] Maddalena Toma,[a] Giovanna Ilaria Passeri,[a] Gualtiero Milani,[a] Angelo Lovece,[a] Alessia Catalano,[a] Claudio Bruno,[a] Annalisa De Palma,[d] Filomena Corbo,[a] Carlo Franchini,[a] Solomon Habtemariam,[e] Giovanni Lentini.[a]

[a]*Department of Pharmacy – Pharmaceutical Sciences, University of Bari Aldo Moro, via E. Orabona n. 4, 70126 Bari, Italy.*

[b]*Department of Pharmacy and Biotechnologies, Alma Mater Studiorum-University of Bologna, Via Belmeloro 6, Bologna, 40126, Italy*.

[c] *Department of Biomedical Sciences and Human Oncology, University of Bari Aldo Moro, Policlinico, piazza Giulio Cesare, 70126 Bari, Italy*

[d]*Department of Biosciences, Biotechnologies, and Biopharmaceutics, University of Bari Aldo Moro, via E. Orabona 4, 70126 Bari, Italy.*

[e]*Pharmacognosy Research Laboratories & Herbal Analysis services UK, University of Greenwich, Chatham-Maritime, Kent ME4 4TB, UK.*

Abstract: Under the hypothesis that cardioprotecting agents might benefit from a synergism between antiarrhythmic activity and antioxidant properties, a small series of mexiletine analogues were coupled with the 2,2,5,5-tetramethylpyrroline moiety, known for its antioxidant effect, in order to obtain dual acting drugs potentially useful in the protection of the heart against post ischemic reperfusion injury. The pyrroline derivatives reported herein (**2a–e**, Fig. 1) were more potent as antiarrhythmic agents than mexiletine and displayed antioxidant activity.

Keywords: antioxidants, pyrroline, reactive oxygen species, antiarrhythmic, voltage gated sodium channel blockers

*Corresponding author: Prof. Alessia Carocci,
Department of Pharmacy – Pharmaceutical Sciences, University of Bari Aldo Moro, via E. Orabona n. 4, 70126 Bari, Italy, phone number: (+39) 080-5442731; fax number: (+39) 080-5442724, E-mail address: alessia.carocci@uniba.it

Table of contents

Synthesis and evaluation of voltage-gated sodium channel blocking pyrroline derivatives endowed with both antiarrhythmic and antioxidant activities

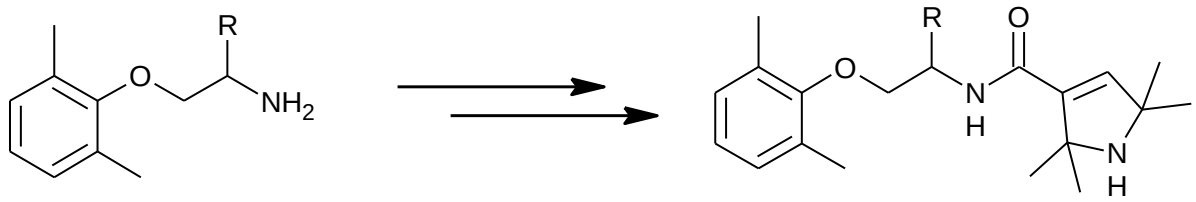

1. Introduction

Due to the presumed role of oxidative stress in a range of human diseases, such as cardiovascular diseases (e.g. atherosclerosis[1,2] and ischemia-reperfusion injury[3]), neurodegenerative disorders[4] (e.g. Alzheimer's[5,6] and Parkinson's diseases[7]), diabetes mellitus,[8] muscular dystrophy,[9] and sepsis,[10] numerous efforts have been focused on the development of new effective antioxidant drugs. Our interest in antioxidants stems from the consideration that mexiletine (**1a**, Figure 1), a well-known voltage-gated sodium channel blocker used in the treatment of myocardial ischemia-related arrhythmias, can also act as an antioxidant by inhibiting hydroxyl radical-mediated lipid peroxidation in brain membranes, probably as a result of a direct interaction of the drug with the biological membranes.[11] Indeed, mexiletine displayed in vivo neuroprotecting properties against oxidative damage associated with diabetes[12] and in a model of focal, neocortal ischemia.[13] Moreover, it has been demonstrated that an increase in the cardioprotective activity of mexiletine is obtained with the introduction of a 2,2,5,5-tetramethylpyrroline structural moiety on the amino group, possibly through the anti-oxidant effect of this moiety.[14,15] In the past decade we have developed several mexiletine analogues with superior potency in blocking skeletal muscle voltage-gated sodium channels than the parent compound.[16,17] Some of these compounds also showed better antiarrhythmic activity along with similar or less cardiovascular effects than mexiletine, thus presenting a higher selectivity of action and reduced side effects.[18] Recently, two tetramethylpyrroline derivatives of both mexiletine and its potent use-dependent isopropyl analogue were tested for their ability to block native $Na_V1.4$ and to exert cytoprotective effects against oxidative-stress injury in myoblasts. Both compounds showed an improved pharmacological profile as sodium channel blockers, with the isopropyl analog being the strongest use-dependent mexiletine-like compound so far, and remarkable cytoprotection at concentrations effective for use-dependent block.[19] Herein, we report the synthesis of the above two pyrroline derivatives (**2a,d**) and of three additional analogs (**2b,c,e**, Figure 1) which were studied for their antiarrhythmic and antioxidant properties.

2. Results and discussion

2.1. Chemistry

Pyrroline derivatives (**2a–e**) were prepared as reported in Scheme 1, following a literature procedure.[20–22] 2,2,6,6-Tetramethylpiperidin-4-one was brominated to obtain the 3,5-dibromo-2,2,6,6-tetramethylpiperidin-4-one hydrobromide (**4**) which was coupled to the appropriate aryloxyalkylamines (**1a–e**)[18] affording the corresponding pyrroline derivatives **2a–e**. Amides **3a–e** were prepared coupling **4** with the appropriate alkylamines.

2.2. Biological results

All the synthesized compounds (**2a–e, 3a–e**) were tested *in vitro* for their antiarrhythmic activity on guinea pig isolated left atria driven at 1 Hz. Results were reported in Table 1 along with data for mexiletine (**1a**) and previously reported mexiletine analogs, amines **1b–e**.[18] Pyrroline derivatives **2a–e** increased the threshold of ac-arrhythmia more than mexiletine did, with the *tert*-butyl derivative **2b** being the most active of the series, with an EC_{50} value in the nanomolar range. Compound **2b** was found to be 215-fold more active than mexiletine, **1a**. Of particular interest, compound **2e** shows an activity of 0.41 μM, which was 10- and 28-fold higher than that of the parent amine **1e** and mexiletine, respectively. It should be noted that, except for compound **2c**, all derivatives were more active than the corresponding parent amines (cfr **2a–e** with **1a–e**, respectively). This result agrees with those previously observed on myoblasts[19] and may be related to the **2a–e** increased lipophilicity (cf. Table 5). While pK_a values were substantially unchanged throughout the three compounds series, Log $D_{7.4}$ values spanned a three order of magnitude range thus reflecting corresponding variations in Log *P* values. Despite possible overestimation,[19] the observed positive relationship between lipophilicity and antiarrhythmic potency agreed with previous observations.[18,19] The elongation of the intermediate chain connecting the aryloxy moieties to the basic functional groups may also be beneficial.[19,23,24] Furthermore, the tetramethylpyrroline basic nitrogen is inserted in a lipophilic structural environment and, when protonated, distributes the cationic charge in the form of partial

charges delocalized on the surrounding carbon atoms.[19] In agreement with previously reported results,[16,19] the cationic charge delocalization is beneficial in mexiletine-like sodium channel blocking agents. Finally, the possible additional contribution of hydrogen bond interactions at the carboxamido group should not be discarded. Being this hypothesis true, the size of the substituents at the chiral center might hinder efficacious hydrogen bond formation. The observed scale of potencies does not support the hypothesis since the antiarrhythmic effect was positively related to the size of the substituent onto the asymmetric center. On the other hand, the partially impaired rotation around the amide bond might be conditioned by steric and electronic effects played by the same substituents. This, in turn, might alter the conformer population distribution with the *s-cis/s-trans* equilibrium more or less pending in favor of the latter. Being a proper orientation of the NHCO group required for efficacious binding, *s-cis/s-trans* equilibrium variations should reflect into corresponding variations in the observed EC_{50} value output. To explore the above hypothesis, a systematic conformational search was performed on **2a–e** through hybrid density functional theory (DFT) B3LYP calculations with the 6-31G* basis set. Following previously developed procedures,[16 25] we generated several conformers in a window of 5 kcal/mol from the global minimum conformation (HF/6-31G*//HF/6-31G*) for each congener in the series **2a–e**. Each conformer of the so-obtained conformer populations underwent geometry optimization at the DFT B3LYP/6-31G* level.[26] The so-obtained conformations were true conformers (no IR imaginary frequencies). Interestingly (Table 2), the most active congeners **2b** and **2e** displayed the higher percentages of *s-cis* forms (14% and 4%, respectively). This observation would suggest that the carboxamide geometry might contribute to the pharmacological output.

Among amides **3a–e,** lacking the 2,6-dimethylphenoxy moiety, only the benzyl derivative **3e** showed an anti-arrhythmic activity comparable to that of mexiletine, though it was less active than the corresponding derivative **2e**. This result suggests the importance of the presence of the 2,6-dimethylphenoxy moiety for the antiarrhythmic activity. Conceivably, the activity of compound **2e** is to be attributed to the presence of the benzyl substituent that takes the place of the missing 2,6-dimethylphenoxy moiety.

In general, amides **3a–e** resulted considerably less potent than the corresponding **2a–e** analogues so that their EC_{50} values have not been determined. The only exception is the benzyl derivative **3e** showing an anti-arrhythmic activity comparable to that of mexiletine (**1a**). Conceivably, the benzyl moiety of **3e** replaces the 2,6-dimethylphenoxy moiety of **1a** during the binding with the target, thus making the two molecules capable of establishing the same binding interactions. However, we speculate that the *tert*-butyl amide **3b** is an interesting compound since it displayed an ac-arrhythmia threshold increase of about 50% at a concentration (0.5 μM) lower than those of all other analogues. Therefore, although less potent than derivatives **2a–e**, amides **3a–e** displayed the same trend of activity, with the *tert*-butyl and benzyl analogues (**2b,e** and **3b,e**) being the more potent of the corresponding series. Conversely, compounds **1a–e**, devoid of the tetramethylpyrroline moiety, showed a completely different binding behavior, with the phenyl analogue **1c** being the most potent. This finding suggests that the presence of the tetramethylpyrroline moiety could force the two series **2a–e** and **3a–e** to establish the same binding poses within the target receptor. On the other hand, the differences in potency hierarchy found between the two series (**2b** > **2e** > **2c** ≅ **2d** ≅ **2a** vs. **1c** > **1b** ≅ **1e** > **1a** ≅ **1d**) suggest that the amides **2a–e** and **3a–e** would share some binding sites with the precursor **1a–e** series but some differences in binding may be taken into account, with the carboxamide group playing a major role (see above). To further explore the contribution of each constituting moiety, a group efficiency (GE = ΔΔG/Δnumber of non-hydrogen atoms = $\Delta 1.37 pEC_{50}/\Delta HA$)[27,28] analysis on **2e** was performed (Figure 2). Three mains putative pharmacophoric elements were captured — the xylyloxy substituent, the tetramethylpyrroline ring, and the substituent at the asymmetric carbon atom — and were color coded in red, green, and blue, respectively. The GE analysis indicated that the substituent on the chiral center gave the highest contribution (GE = 0.26) while the tetramethylpyrroline ring displayed the lowest GE value (0.14). This could mean that the non-hydrogen atoms (HA) constituting the latter moiety contribute less efficiently to the binding of **2e** with respect to the xylyloxy and the phenyl substituents (GE = 0.26 and 0.22, respectively). In Figure 3, the global minimum conformer electrostatic potential maps (DFT

B3LYP/6-31G*//DFT B3LYP/6-31G*) of compounds **2a–e** are captured in a cartoon representing all pharmacophoric elements discussed so far interacting with corresponding hypothetical binding sites. In particular, we suggest that the substituent at the chiral center would be recognized by a roughly spherical pocket that would be fully occupied by the *tert*-butyl group (**2b**) while resulting relatively large (**2a**, **2c**, and **2d**) or narrow (**2e**) for the other substituents. The cartoon might also explain why **2c** is the only tetramethylpyrroline derivative less active than the parent compound (**1c**): it may be hypothesised that the contemporary presence of three contiguous, flat and rigid moieties (viz., phenyl substituent, amide group, and tetramethylpyroline ring) impedes the correct fit for compound **2c**.

To better define the cardiac profile of the pyrroline derivatives, their influence on additional cardiac parameters was compared with that elicited by the reference compound, mexiletine (**1a**) (Table 3). Pyrroline derivatives **2a–e** decreased the developed tension on driven left atria less than mexiletine did, except for the isopropyl derivative **2d** whose effect was comparable with that of mexiletine. On the other hand, the corresponding amides **3a–e** showed a strong activity with EC_{50} values within the range of 0.0019 and 0.11 μM. The most potent compound was **3b** showing a negative inotropism 24-fold higher than that of mexiletine. Regarding the negative chronotropic activity on spontaneously beating right atrium, only compounds **2b** and **2c** showed a weak activity, which was 55-fold and 130-fold lower than that of mexiletine. Furthermore, almost all compounds showed negative inotropism on spontaneously beating right atrium even though with different degree of potency, ranging from 0.049 μM for **3c** to 1.48 μM for **2a**. It is noteworthy that this effect was not recorded for mexiletine and compounds **2b** and **2c** due to their insignificant inotropism resulting from chronotropic effect. Moreover, all the new pyrroline derivatives were tested on K^+-depolarized (80 mM KCl) guinea pig aortic strips to assess their vasorelaxant activity. Data are shown in Table 4 with mexiletine as the reference drug. For all compounds, the intrinsic vasorelaxant activity percentage on aorta was lower than 30% and thus unremarkable. In order to rule out a possible inhibitory effect on nonvascular smooth muscle, such as that displayed by Ca^{2+} channel antagonists, further investigation on relaxant activity using K^+-depolarized (80 mM KCl) guinea pig ileum longitudinal smooth muscle (GPILSM)

was pursued (Table 4). With regards to the pyrroline derivatives **2a–e**, the observed profile of intrinsic activity and potency for **2a** and **2d** was substantially similar to that displayed by mexiletine, while compounds **2b**, **2c** and **2e** showed a relaxant potency slightly higher than that of mexiletine, but in the micromolar range. Overall, all pyrroline derivatives **2a–e** appears to display a higher intrinsic activity in nonvascular than vascular smooth muscle cells. The effect of these compounds on guinea pig ileum longitudinal smooth muscle suggests a conceivable involvement of L-type calcium channels.

Notably, among the newly synthesized compounds, **2b** and **2e** were the most interesting mexiletine derivatives since they displayed both the highest antiarrhythmic activity and the best cardiovascular profile, showing both negative inotropism and cronotropism lower than the parent compound and a negligible vasorelaxant activity on guinea-pig aortic strips. Thus, they were tested *in vitro* on voltage gated sodium currents recorded in HEK293 cells transiently transfected with the human cardiac sodium channel, hNav1.5, using the whole-cell patch-clamp method, in order to investigate the contribution of the block of this channel to the observed antiarrhythmic activity. Both the compounds produced a concentration- and use-dependent inhibition of sodium currents (Figure 3). Compared to the reference compound, mexiletine, tonic block measured at 0.1 Hz frequency was increased about two-fold for **2e** and four-fold for **2b** (Table 5). However, **2e** was more use-dependent than mexiletine and **2b** were; the IC_{50} ratios were similar for mexiletine and **2b**, whereas those of **2e** were greater by 4.5-fold and about 7-fold at 2 and 10 Hz, respectively, than those of **2b**. Conceivably, increased lipophilia of the tested compounds, compared to that of mexiletine (Table 6), may contribute to the increased tonic block exerted by the two compounds. Such a behavior was observed with other compounds containing two aromatic rings, such as diphenylhydramine and orphenadrine.[29,30] These results are in line with what was found in our previous studies.[31,32] The increased use-dependence of **2e** suggests a stronger interaction with the sodium channel in the inactivated state. Since the hierarchy of potency on $Na_V1.5$ (**2e** > **2b**) appeared as opposite to that observed in the antiarrhythmic activity assay (**2b** > **2e**), the sodium channel blocking activity of our mexiletine derivatives, while possibly

contributing to the observed cardiac effects, is not sufficient to completely interpret the pharmacological profile of **2a–e**.

The *in vitro* antioxidant activity of the compounds under study (**2a–e, 3a–e**) was evaluated by means of the *2′,7′*-dichlorodihydrofluorescein diacetate (DCFH-DA) cellular-based assay by measuring the reducing effect of the test compounds against oxidation of *2′,7′*-dichlorodihydrofluorescein (DCFH) to the fluorescent probe *2′,7′*-dichlorofluorescein (DCF). Mexiletine was chosen as reference compound. Results are reported in Table 7. Tests were performed on human hepatocellular liver carcinoma (HepG2) cells because they have an enhanced oxidative metabolism that causes cellular oxidative stress and/or generates reactive metabolites. Thus, it may be assumed that HepG2 cells are suited to study protection against oxidative and cytotoxic effects, if any. The results of the DCFH-DA assay showed that all pyrroline derivatives **2a–e** significantly reduce the H_2O_2-induced oxidation, being slightly more potent than mexiletine. Conversely, none of the amides **3a–e** did show any appreciable antioxidant activity. Based on these results it is possible to assume that the 2,6-dimethylphenoxy moiety is crucial for the antioxidant activity as well as for the antiarrhythmic one.

Finally, the ability of mexiletine and some synthesized compounds (**2a–d**, **3a**) to react against hydroxyl radical using the antioxidant-sensitive non fluorescent probe benzoic acid in the presence of hydroxyl radicals was measured. The results revealed that all tested compounds scavenge hydroxyl radicals (IC_{50} about 70 μM), being slightly more active than mexiletine (IC_{50} 93 ± 9 μM). The same test run on **3a** (IC_{50} 198 ± 4μM) underlines once again the importance of the 2,6-dimethylphenoxy moiety in the biological profile of such compounds.

3. Conclusion

Highly lipophilic amines are generally feared as possible pro-arrhythmic agents due to possible interaction with the human ether-a-go-go-related gene (hERG) channel with the potency of hERG blocking agents being generally related to MW and lipophilicity.[33] Curiously, the tetramethylpyrroline derivatives reported herein performed as potent antiarrhythmic agents. The

observed activities were probably related to the block of cardiac sodium and calcium channels. The most interesting tetramethylpyrroline congener was the *tert*-butyl-substituted analog **2b** which was at least 100 times more active as an antiarrhythmic than our lead compound mexiletine (**1a**). Interestingly, **2b** presents the highest fraction of sp^3 hybridised carbon atoms (Fsp^3) in the congeneric series **2a–e**. A four-point interaction with voltage-gated sodium and calcium channels was supposed to account for the observed antiarrhythmic activity, with the latter probably playing a major role. This implies that chirality may offer a way to further improve the pharmacological profile of the stated compounds. Both high Fsp^3 and the presence of chiral centers have been related to clinical developability.[26,34] The group efficiency (GE) analysis indicated the aryloxy moiety as a pharmacophoric group and we have previously reported that the introduction of a hydroxyl group onto the 3-position of the aromatic ring of mexiletine improves potency on voltage-gated sodium channels [29] while reducing the feared blocking activity on hERG.[35] Interestingly, the 3-hydroxy analog of mexiletine displayed stereoselectivity of action as an antiarrhythmic (*R* > *S*).[36] Since **2a–e** displayed antioxidant activity, this series of mexiletine derivatives may be considered as a starting point toward the development of dual-acting drugs designed to obtain a combined activity on arrhythmias in the ischemic heart.

4. Experimental protocols

4.1. Chemistry

Chemicals were purchased from Sigma-Aldrich or Lancaster. Yields refer to purified products and were not optimized. The structures of the compounds were confirmed by routine spectrometric and spectroscopic analyses. Only spectra for compounds not previously described are given. Melting points were determined on a Gallenkamp apparatus in open glass capillary tubes and are uncorrected. ^{1}H NMR and ^{13}C NMR spectra were recorded on either a Varian VX Mercury spectrometer operating at 300 and 75 MHz for ^{1}H and ^{13}C, respectively, or an AGILENT 500 MHz operating at 500 and 125 MHz for ^{1}H and ^{13}C, respectively, using $CDCl_3$ and CD_3OD as solvents. Chemical shifts (δ) are

reported in ppm relative to the residual non-deuterated solvent resonance: $CDCl_3$, δ = 7.26 (^{1}H NMR) and δ = 77.3 (^{13}C NMR); CD_3OD, δ = 3.30 (^{1}H NMR) and δ = 47.8 (^{13}C NMR) as internal references. Coupling constants (*J*) are given in Hz. Gas chromatography (GC)/mass spectroscopy (MS) was performed on a Hewlett-Packard 6890–5973 MSD at low resolution. Liquid chromatography (LC)/mass spectroscopy (MS) was performed on a spectrometer Agilent 1100 series LC-MSD Trap System VL. Elemental analyses were performed on a Eurovector Euro EA 3000 analyzer and the data for C, H, N were within ± 0.4 of theoretical values. Chromatographic separations were performed on silica gel columns by column chromatography on silica gel (Kieselgel 60, 0.040–0.063 mm, Merck, Darmstadt, Germany) as described by Still et al.[37] TLC analyses were performed on precoated silica gel on aluminium sheets (Kieselgel 60 F_{254}, Merck).

3,5-Dibromo-2,2,6,6-tetramethylpiperidin-4-one (4)

The title compound was prepared according to the literature procedure.[20] To a solution of 2,2,6,6-tetramethylpiperidin-4-one (2.0 g) in 10 ml of glacial acetic acid a solution of Br_2 in 8 ml of glacial acetic acid was added dropwise. The reaction mixture was heated at 60 °C overnight. Then the reaction mixture was filtered and the solid was washed with acetic acid, H_2O and finally with Et_2O. After dried at room temperature for 15 days, a white solid (3.712 g) was obtained: yield 73%; mp: > 250 °C ; ^{1}H NMR (300 MHz, CD_3OD): δ 1.45 (s, 6H, CH_3), 1.83 (s, 6H, CH_3), 5.47 (s, 2H, CH); ^{13}C NMR (75 MHz, CD_3OD): δ 22.9 (2C), 28.0 (2C), 59.1 (2C), 65.85 (2C), 189.1 (1C). Other spectroscopic data were in agreement with the literature.[20]

2,2,5,5-Tetramethyl-*N*-[1-(2,6-dimethylphenoxy)propan-2-yl]-2,5-dihydro-1*H*-pyrrole-3-carboxamide (2a) To a solution of **1a·HCl** (0.300 g, 1.4 mmol) in 10 mL of water, cooled in an ice bath, trimethylamine (0.495 g, 4.9 mmol) was added. After removing the ice bath, 3,5-dibromo-2,2,6,6-tetramethylpiperidin-4-one **(4)** (0.700 g, 1.7 mmol) was added in small portions over a period of 6 hours. The reaction mixture was stirred at 50 °C for 24 h, then it was made alkaline with 6N

NaOH and extracted with EtOAc. Removal of the solvent under vacuo gave 0.500 g (61%) of **2a** as a yellow solid which was recrystallized from EtOAc/hexane. White crystals: yield: 61%; mp: 131–132 °C (EtOAc/hexane). GC-MS (70 eV) *m/z* (%) 315 (M^+ –15, 45), 110 (100). ^{1}H NMR (300 MHz, $CDCl_3$): δ 1.44–1.50 (m, 9H, $2CH_3C$ + CH_3CH), 1.62 (d, *J* = 3.9 Hz, 6H, $2CH_3C$), 2.26 (s, 6H, CH_3Ar), 2,95 (br s, 1H, NH), 3.74 (dd, *J* = 3.0, 9.1 Hz, 1H, C*H*H), 3.86 (dd, *J* = 3.9, 9.1 Hz, 1H, CH*H*), 4.36–4.41 (m, 1H, $CHCH_2$), 6.07 (s, 1H, CH), 6.26 (br d, *J* = 8.3 Hz, 1H, NHCO), 6.93 (t, *J* = 7.3 Hz, 1H, CHAr), 7.01 (d, *J* = 7.2 Hz, 2H, CHAr); ^{13}C NMR (75 MHz, $CDCl_3$): δ 16.4 (2C), 18.3 (1C), 30.3 (4C), 45.4 (1C), 63.9 (1C), 67.5 (1C), 74.0 (1C), 124.4 (1C), 129.3 (2C), 130.9 (2C), 140.2 (1C), 143.5 (1C), 155.0 (1C), 164.6 (1C). Anal. ($C_{20}H_{30}N_2O_2 \cdot 0.5H_2O$) C, H, N.

2,2,5,5-Tetramethyl-*N*-[3,3-dimethyl-1-(2,6-dimethylphenoxy)butan-2-yl)-2,5-dihydro-1*H*-pyrrole-3-carboxamide (2b)

White crystals: mp 87–88 °C (EtOAc/hexane); GC-MS (70 eV) *m/z* (%) 357 (M^+, –15, 100); ^{1}H NMR (300 MHz, $CDCl_3$): δ 1.08 (s, 9H, CH_3C), 1.30 (d, *J* = 6.3 Hz, 6H, CH_3CNH), 1.42 (s, 6H, CH_3CNH), 1.49 (s, 6H, CH_3CNH), 1.78 (br s, 1H, NH), 2.15 (s, 6H, CH_3Ar), 3.75 (dd, *J* = 9.6, 3.9 Hz, 1H, C*H*H), 4.02 (dd, *J* = 9.9, 3.8 Hz, 1H, CH*H*), 4.06–4.97 (m, 1H, $CHCH_2$), 6.11 (s, 1H, CH), 6.33 (br d, *J* = 8.9 Hz, 1H, NHCO), 6.90–6.99 (m, 3H, CHAr); ^{13}C NMR (75 MHz, $CDCl_3$): δ 16.9 (2C), 27.6 (3C), 30.1 (2C), 30.3 (2C), 34.9 (1C), 56.5 (1C), 64.3 (1C), 67.9 (1C), 71.3 (1C), 124.4 (1C), 129.3 (2C), 130.8 (2C), 139.2 (1C), 143.8 (1C), 155.5 (1C), 164.9 (1C). Anal. ($C_{23}H_{36}N_2O_2 \cdot 0.5H_2O$) C, H, N.

2,2,5,5-Tetramethyl-*N*-[2-(2,6-dimethylphenoxy)-1-phenylethyl]-2,5-dihydro-1*H*-pyrrole-3-carboxamide (2c)

Yellow crystals: mp 133–134 °C (EtOAc/petroleum ether); GC-MS (70 eV) *m/z* (%) 377 (M^+ –15, 52), 110 (100). ^{1}H NMR (300 MHz, $CDCl_3$): δ 1.33 (s, 6H, CH_3C), 1.48 (d, *J* = 3.9 Hz, 6H, CH_3C), 2.11 (s, 7H, CH_3Ar + NH), 4.03 (dd, *J* = 9.6, 4.1 Hz, 1H, C*H*H), 4.12 (dd, *J* = 9.4, 4.4 Hz, 1H, CH*H*),

5.34–5.44 (m, 1H, $CHCH_2$), 6.19 (s, 1H, CH), 6.78 (br d, *J* = 8.0 Hz, 1H, NHCO), 6.90–6.99 (m, 3H, CHAr), 7.31–7.47 (m, 5H, CHAr); ^{13}C NMR (75 MHz, $CDCl_3$): δ 16.4 (2C), 30.3 (2C), 30.4 (2C), 53.4 (1C), 63.9 (1C), 67.4 (1C), 74.1 (1C), 124.5 (1C), 127.1 (2C), 128.0 (2C), 128.9 (1C), 129.3 (2C), 130.9 (2C), 139.7 (1C), 140.8 (1C), 143.4 (1C), 155.0 (1C), 164.7 (1C). Anal. ($C_{25}H_{32}N_2O_2 \cdot 05H_2O$) C, H, N.

2,2,5,5-Tetramethyl-*N*-[1-(2,6-dimethylphenoxy)-3-methylbutan-2-yl]-2,5-dihydro-1*H*-pyrrole-3-carboxamide (2d)

White crystals: mp 96–97 °C (EtOAc/hexane); GC-MS (70 eV) *m/z* (%) 343 (M^+ –15, 60), 110 (100). ^{1}H NMR (500 MHz, $CDCl_3$): δ 1.05 (d, *J* = 4.1 Hz, 3H, CH_3CHCH_3), 1.11 (d, *J* = 3.8 Hz, 3H, CH_3CHCH_3), 1.32 (d, *J* = 4.7 Hz, 6H, CH_3C), 1.47 (s, 3H, CH_3C), 1.50 (s, 3H, CH_3C), 2.18–2.23 (m, 1H, $CHCH_3$), 3.78 (dd, *J* = 9.3, 3.9 Hz, 1H, C*H*H), 3.99 (dd, *J* = 9.3, 2.9 Hz, 1H, CH*H*), 4.02–4.05 (m, 1H, $CHCH_2$), 6.09 (s, *1*H, CH), 6.25 (br d, *J* = 9.3 Hz, 1H, NHCO), 6.93 (t, *J* = 7.6 Hz, 1H, CHAr), 7.00 (d, *J* = 7.3 Hz, 2H, CHAr); ^{13}C NMR (125 MHz, $CDCl_3$): δ 16.4 (2C), 19.3 (1C), 20.0 (1C), 29.3 (2C), 30.1 (2C), 30.2 (1C), 54.5 (1C), 63.7 (1C), 67.3 (1C), 71.2 (1C), 124.2 (1C), 129.1 (2C), 130.6 (2C), 139.5 (1C), 143.6 (1C), 155.0 (1C), 164.7 (1C). Anal. ($C_{22}H_{34}N_2O_2 \cdot 0.5H_2O$) C, H, N.

2,2,5,5-Tetramethyl-*N*-[1-(2,6-dimethylphenoxy)-3-phenylpropan-2-yl)-2,5-dihydro-1*H*-pyrrole-3-carboxamide (2e)

White crystals: mp 159–160°C (EtOAc/hexane); GC-MS (70 eV) *m/z* (%) 391 (M^+ –15, 32), 110 (100). ^{1}H NMR (500 MHz, $CDCl_3$): δ 1.32 (s, 6H, CH_3C), 1.41 (s, 3H, CH_3C), 1.44 (s, 3H, CH_3C), 2.26 (s, 6H, CH_3Ar), 3.16 (d, *J* = 7.3 Hz, 2H, CH_2Ar), 3.80–3.88 (m, 2H, CH_2CH), 4.54–4.62 (m, 1H, CH), 5.97 (s, 1H, NH), 6.23 (br d, *J* = 8.3 Hz, 1H, NHCO), 6.93 (t, *J* = 6.6 Hz, 1H, CHAr), 7.00 (d, *J* = 7.8 Hz, 2H, CHAr), 7.21–7.27 (m, 2H, CHAr), 7.28–7.34 (m, 3H, CHAr); ^{13}C NMR (125 MHz,

$CDCl_3$): δ 16.4 (2C), 29.8 (2C), 29.9 (2C), 37.7 (1C), 50.5 (3C), 71.7 (1C), 124.2 (1C), 126.7 (1C), 128.6 (2C), 129.1 (2C), 129.2 (2C), 130.6 (2C), 137.7 (1C), 139.6 (2C), 143.2 (2C), 154.9 (1C), 164.5 (1C). Anal. ($C_{26}H_{34}N_2O_2 \cdot 0.5H_2O$) C, H, N.

2,2,5,5-Tetramethyl-*N*-(propan-2-yl)-2,5-dihydro-1*H*-pyrrole-3-carboxamide (3a)

White crystals: mp 147–148 °C (EtOAc/hexane); GC-MS (70 eV) *m/z* (%) 195 (M^+ –15, 4), 110 (100); ^{1}H NMR (300 MHz, CD_3OD): δ 1.18 (d, *J* = 6.6 Hz, 6H, *CH*$_3$CH), 1.62 (s, 6H, *CH*$_3$C), 1.71 (s, 6H, *CH*$_3$C), 3.95–4.12 (m, 1H, *CH*CH_3), 6.38 (s, 1H, CH); ^{13}C NMR (75 MHz, CD_3OD): δ 21.2 (2C), 26.0 (2C), 26.2 (1C), 41.5 (1C), 68.5 (1C), 71.9 (1C), 135.7 (1C), 138.7 (1C), 162.4 (1C). Anal. ($C_{12}H_{22}N_2O$) C, H, N.

2,2,5,5-Tetramethyl *N*-(3,3-dimethylbutan-2-yl)-2,5-dihydro-1*H*-pyrrole-3-carboxamide (3b)

White crystals: mp 96–98 °C (EtOAc/hexane); GC-MS (70 eV) *m/z* (%) 286 (M^+ –15, 3), 110 (100); ^{1}H NMR (500 MHz, $CDCl_3$): δ 0.91 (s, 9H, *CH*$_3$C), 1.08 (d, *J* = 6.8 Hz, 3H, *CH*$_3$CH), 1.29 (s, 6H, *CH*$_3$CN), 1.43 (d, *J* = 4.9 Hz, 6H, 2*CH*$_3$CH), 1.85 (br s, 1H, NH), 3.90–3.97 (m, 1H, *CH*CH_3), 5.52 (br d, *J* 9.3 Hz, 1H, NHCO), 5.99 (s, 1H, CH); ^{13}C NMR (125 MHz, $CDCl_3$): δ 16.2 (1C), 26.2 (3C), 30.1 (2C), 30.2 (2C), 34.3 (1C), 52.3 (1C), 63.5 (1C), 67.0 (1C), 139.0 (1C), 144.1 (1C), 164.6 (1C). Anal. ($C_{15}H_{28}N_2O \cdot 0.33H_2O$) C, H, N.

2,2,5,5-Tetramethyl-*N*-(1-phenylethyl)-2,5-dihydro-1*H*-pyrrole-3-carboxamide (3c)

White crystals: mp 145–147°C (EtOAc/hexane); GC-MS (70 eV) *m/z* (%) 257 (M^+ –15, 3), 110 (100); ^{1}H NMR (300 MHz, $CDCl_3$): δ 1,26 (d, *J* = 4.1 Hz, 6H, *CH*$_3$C), 1,42 (d, *J* = 6.1 Hz, 6H, *CH*$_3$C), 1,52 (d, *J* = 6.9 Hz, 3H, *CH*$_3$CH), 1.76 (br s, 1H, *NH*), 5.08–5.22 (m, 1H, *CH*CH_3), 5.98 (br d, *J* 7.4 Hz, 1H, NHCO), 6.03 (s, 1H, CH), 7.22–7.40 (m, 5H, CHAr); ^{13}C NMR (75 MHz, $CDCl_3$): δ 22.0 (1C),

30.4 (2C), 30.5 (2C), 48.8 (1C), 63.7 (1C), 67.3 (1C), 126.4 (1C), 127.6 (2C), 129.0 (2C), 140.1 (1C), 143.4 (1C), 143.7 (1C), 164.5 (1C). Anal. ($C_{17}H_{24}N_2O \cdot 0.33H_2O$) C, H, N.

2,2,5,5-Tetramethyl-*N*-(3-methylbutan-2-yl)-2,5-dihydro-1*H*-pyrrole-3-carboxamide (3d)

White crystals: mp 126–127 °C (EtOAc); GC-MS (70 eV) *m/z* (%) 238 (M^+ –15, 25), 110 (100); ^{1}H NMR (300 MHz, $CDCl_3$): δ 0.90 (dd, *J* = 6,8, 1.8 Hz, 6H, *CH*$_3$CH), 1.09 (d, *J* = 6.9 Hz, 3H, *CH*$_3$CHN), 1.27 (s, 6H, *CH*$_3$C), 1.42 (d, 6H, *J* = 1.9 Hz, *CH*$_3$C), 1.78 (br s, 1H, NH), 3.80–3.98 (m, 1H, *CH*CH$_3$), 5.52 (br d, *J* 8.3 Hz, 1H, NHCO), 5.99 (s, 1H, CH); ^{13}C NMR (75 MHz, $CDCl_3$): δ 17.6 (1C), 18.7 (1C), 18.8 (1C), 30.3 (1C), 30.4 (1C), 30.5 (2C), 33.3 (1C), 49.9 (1C), 63.7 (1C), 67.2 (1C), 139.4 (1C), 144.2 (1C), 164.9 (1C). Anal. ($C_{14}H_{26}N_2O$) C, H, N.

2,2,5,5-Tetramethyl-*N*-(1-phenylpropan-2-yl)-2,5-dihydro-1*H*-pyrrole-3-carboxamide (3e)

White crystals: mp 149–150°C (EtOAc/hexane); GC-MS (70 eV) *m/z* (%) 271 (M^+ –15, 79), 110 (100); ^{1}H NMR (500 MHz, $CDCl_3$): δ 1.15 (d, *J* = 6,4 Hz, 3H, *CH*$_3$CH), 1.27 (d, *J* = 2.9 Hz, 6H, *CH*$_3$C), 1.40 (s, 6H, *CH*$_3$C), 1.93 (br s, 1H, NH), 2.77 (dd, *J* = 13.7, 7.3 Hz, 1H, C*H*H), 2.86 (dd, *J* = 13.5, 5.7 Hz, 1H, CH*H*), 4.27–4.33 (m, 1H, *CH*CH$_3$), 5.53 (br d, *J* = 7.8 Hz, 1H, NHCO), 5.92 (s, 1H, *CH*CN), 7.18–7.26 (m, 3H, *CH*Ar), 7.28–7.31 (m, 2H, *CH*Ar); ^{13}C NMR (125 MHz, $CDCl_3$): δ 20.0 (1C), 30.0 (2C), 30.1 (2C), 42.3 (1C), 45.9 (1C), 63.5 (1C), 67.0 (1C), 126.5 (1C), 128.4 (1C), 129.5 (1C), 137.9 (2C), 139.5 (2C), 143.6 (1C), 164.5 (1C). Anal. ($C_{18}H_{26}N_2O \cdot 0.25H_2O$) C, H, N.

4.2. Pharmacology

4.2.1. **Details for functional studies**

The pharmacological profile of all compounds was derived on guinea-pig isolated left and right atria to evaluate their inotropic and/or chronotropic effects, respectively, and on K^+-depolarized (80 mM) guinea-pig vascular (aortic strips) and non-vascular [ileum longitudinal smooth muscle (GPILSM)] to assess the calcium antagonist activity. The antiarrhythmic activity of all compounds was tested on isolated guinea pig left atria driven at 1 Hz. Compounds were checked at increasing doses to evaluate: i) antiarrhythmic activity, inducing arrhythmias by application of sinusoidal alternating current (50 Hz) of increasing strength to the isolated left atria driven at 1 Hz and assessing the "threshold of ac-arrhythmia" (the current strength at which extra beats occurs) before and following the compound was added to the tissue bath[38], ii) the percent decrease of developed tension on isolated left atrium driven at 1 Hz and on spontaneously beating right atrium (negative inotropic activity), iii) the percent decrease in atrial rate on spontaneously beating right atrium (negative chronotropic activity), and iv) the percent inhibition of calcium-induced contraction on K^+-depolarized aortic strips and GPILSM (vascular and non-vascular relaxant activity respectively). Details have been reported on supporting information. Data were analyzed using Student's *t*-test and are presented as mean ± S.E.M.[39] Since the analyzed compounds were added in cumulative manner, the difference between the control and the experimental values at each concentration were tested for a P value < 0.05. The potency of drugs defined as EC_{50} and IC_{50} was evaluated from log concentration-response curves (Probit analysis using Litchfield and Wilcoxon[39] or GraphPad Prism® software.[40,41]

4.2.2. **Details for patch clamp experiments.**

Effects of compounds on human cardiac sodium channels were investigated as previously described.[29,42] Transient transfection of the HEK293 cells (human embryonic kidney cell line) was achieved using the calcium-phosphate co-precipitation method. The cells were incubated for 24 hours with 0.1 µg/ml of the full-length *SCN5A* cDNA, encoding the α-subunit of the human cardiac sodium channel subtype hNav1.5, and 0.05 µg/ml of a plasmid expressing the CD8 receptor and the auxiliary

human voltage-gated sodium channel β_1 subunit (pCD8-IRES-hβ1). Cells marked with anti-CD8 antibody-coated microbeads (Dynal-Invitrogen, Milan, Italy) were used for patch clamp experiments 48−72 h after transfection. Whole-cell sodium currents were recorded at room temperature (20−22 °C) using Axopatch-1D amplifier (Axon Instruments Inc., Union City, CA, USA) and pClamp suite software (Axon Instruments). The composition of the bath solution was (mM): 150 NaCl, 4 KCl, 2 $CaCl_2$, 1 $MgCl_2$, 5 HEPES and 5 glucose (pH 7.4). The pipette solution contained (mM): 120 CsF, 10 CsCl, 10 NaCl, 5 EGTA, and 5 HEPES (pH 7.2). With these solutions, pipette resistance was 2-4 mV. After stabilization of the whole-cell configuration, sodium currents were elicited by a 25 ms-long test pulse to -30 mV from a holding potential of −120 mV applied at 0.1, 2, and 10 Hz frequencies. The patched cell was exposed to a continuous stream of control or drug-supplemented bath solution. To limit bias due to rundown and shifts of channel voltage dependence, only two drug concentrations were tested on each cell. The I_{DRUG}/I_{CTRL} ratio (mean ± S.E.M. from 3-8 cells) was reported as a function of drug concentration. The relationships were fitted to a first-order binding function, $I_{drug} / I_{ctrl} = 1/\{1 + ([drug]/IC_{50})^{nH}\}$, allowing the calculation of half-maximum inhibitory concentration (IC_{50}) and slope factor (nH). The fit parameters are given with the standard error of the fit.

4.2.3. **Details for antioxidant activity studies**

4.2.3.1. **Culture cells**

Human hepatocellular liver carcinoma (HepG2) cells (Sigma–Aldrich, St. Louis, MO) were cultured in DMEM-Dulbecco's modified Eagle's medium (Sigma–Aldrich, St. Louis, MO) supplemented with 10% (v/v) inactivated fetal bovine serum (PAA Laboratories GmbH, Pasching, Austria), L-glutamine (2 mM) (Sigma–Aldrich, St. Louis, MO), penicillin (100 μg/ml) and streptomycin (100 μg/ml) (Sigma–Aldrich, St. Louis, MO) and incubated at 37 °C in a humid atmosphere of 5% CO_2. For cell assays, cells were trypsinized using Trypsin-EDTA 1X in PBS (Aurogene) and plated in 96-well plates at a density of 10 000 cells per well in 125 μL of cell culture medium.

4.2.3.2. **Detection of ROS generation**

Generation of ROS was monitored using an oxidation-sensitive fluorescent probe, 2′,7′-dichlorodihydrofluorescein diacetate (DCFH-DA, D6665; Sigma–Aldrich, St. Louis, MO) by slightly modifying the procedure reported by Wang and James.[43] Briefly, viable cells (10^4/well) were seeded in a black 96-well cell culture plate (PerkinElmer USA) and after 24 h were incubated with different concentrations (10–100 μg/ml) of the tested compounds for 2 h at 37 °C in 5% CO_2. DCFH-DA (50 μM final concentration) in medium without serum was added directly to each well, and the plate was incubated at 37 °C for 30 min at 37 °C in 5% CO_2. After washing using PBS, 100 μM H_2O_2 in PBS was added to each well and the cells were incubated for an additional 30 min. The formation of fluorescent dichlorofluorescein (DCF) due to oxidation of DCFH in the presence of ROS, was read at 480 nm using a multilabel plate counter Victor^3 V (PerkinElmer) and DMSO medium was used for control cells. At least three independent experiments with sex replicates were carried out, and the results were averaged. Data were analyzed using Student's *t*-test and are presented as mean ± S.E.M. The mean difference between the control and experimental values at each concentration were tested for a P value < 0.05.

4.2.3.3. **Measurement of hydroxyl radical scavenging activity**

The hydroxyl radical scavenging activity was measured according to the method of Toth *et al*.,[15] with some modifications. Briefly, 3 mL of a solution containing 40 mM sodium phosphate buffer (pH 3), 0.1 mM benzoic acid, 0.02 mM hydrogen peroxide, 0.04 mM Fe(II)-EDTA, and tested compounds (dissolved in DMSO) in different concentrations was incubated for 30 min at 37 °C. The fluorescence was then monitored at the excitation wavelength of 305 nm and the emission wavelength of 407 nm by a LS 55 Luminescence spectrometer (Perkin Elmer). All the tests were performed in triplicates and reported as mean values.

4.3. **Quantum mechanical calculations**

The previously developed procedures were followed.[16,19,25,36] Briefly, the models of protonated compounds **2a–e** were generated from the atomic fragments incorporated into Spartan'16 (Wavefunction Inc., Irvine, CA) inner fragment library and assuming the suggested default starting geometries. The generated geometries were optimized by the molecular mechanics MMFF routine offered by the software[44] and then submitted to a systematic conformational distribution analysis using the default step sizes. All conformers in a window of 10 Kcal/mol above the global minimum conformer were retained. When two conformers differed by dihedral values lower than 10°, the less stable conformer was left out. Conformers were then classified according to their ab initio gas phase energy content calculated at the RHF/3-21G*level. All conformers falling within a window of 5 kcal/mol above global minimum were retained and submitted to RHF/3-21G* geometry optimization. After removal of redundant conformers (i.e., each conformer differing from a more stable one by less than 5° in their corresponding dihedral values), the single point energy content for all the remaining conformers were calculated at the RHF/6-31G** level. The so-obtained set of conformers underwent geometry optimization by density functional theory (DFT) implemented in Spartan'16 with B3LYP functional[45] and the 6-31G* basis set[46] in the gas phase. The optimized structures were confirmed as real minima by IR frequency calculation (DFT B3LYP/6-31G*// DFT B3LYP/6-31G*). All simulations were performed in vacuum.

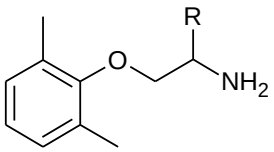

1a-e

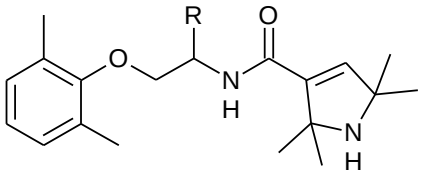

2a-e

a: R = CH_3

b: R = *t*Bu

c: R = Ph

d: R = *i*Pr

e: R = Bn

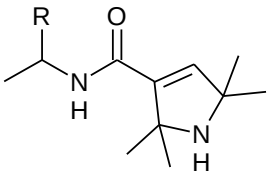

3a-e

Figure 1. Structures of mexiletine analogues (**1a–e**), their pyrroline derivatives (**2a–e**) and amides (**3a–e**).

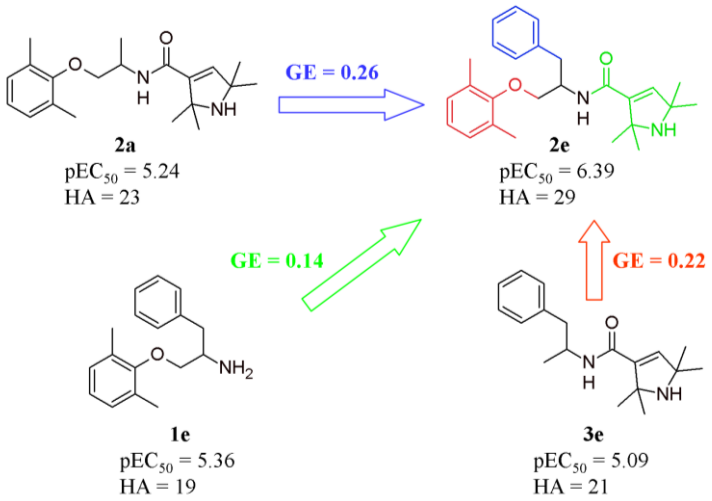

Figure 2. Group efficiency (GE) analysis on **2e**: GE = ΔΔG/Δnumber of non-hydrogen atoms = $\Delta 1.37 pEC_{50}/\Delta HA$.[45]

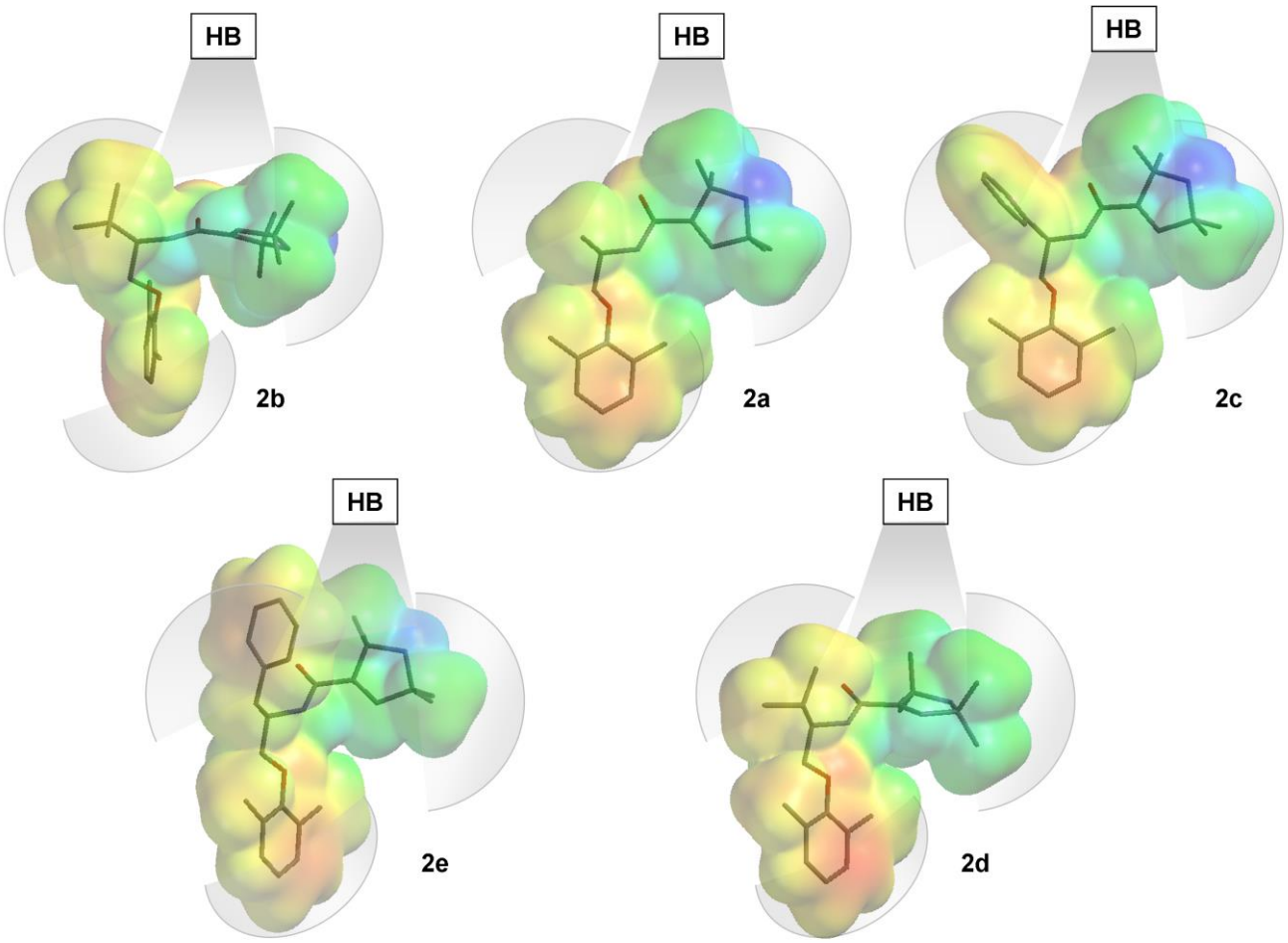

Figure 3. Putative pharmacophoric elements and interacting binding sites for compounds **2a-e** represented as the corresponding most stable conformers wrapped in their electrostatic potential maps (DFT B3LYP/6-31G*//DFT B3LYP/6-31G*); for the sake of simplicity, the homochiral R series only was considered; HB, hydrogen bond forming site.

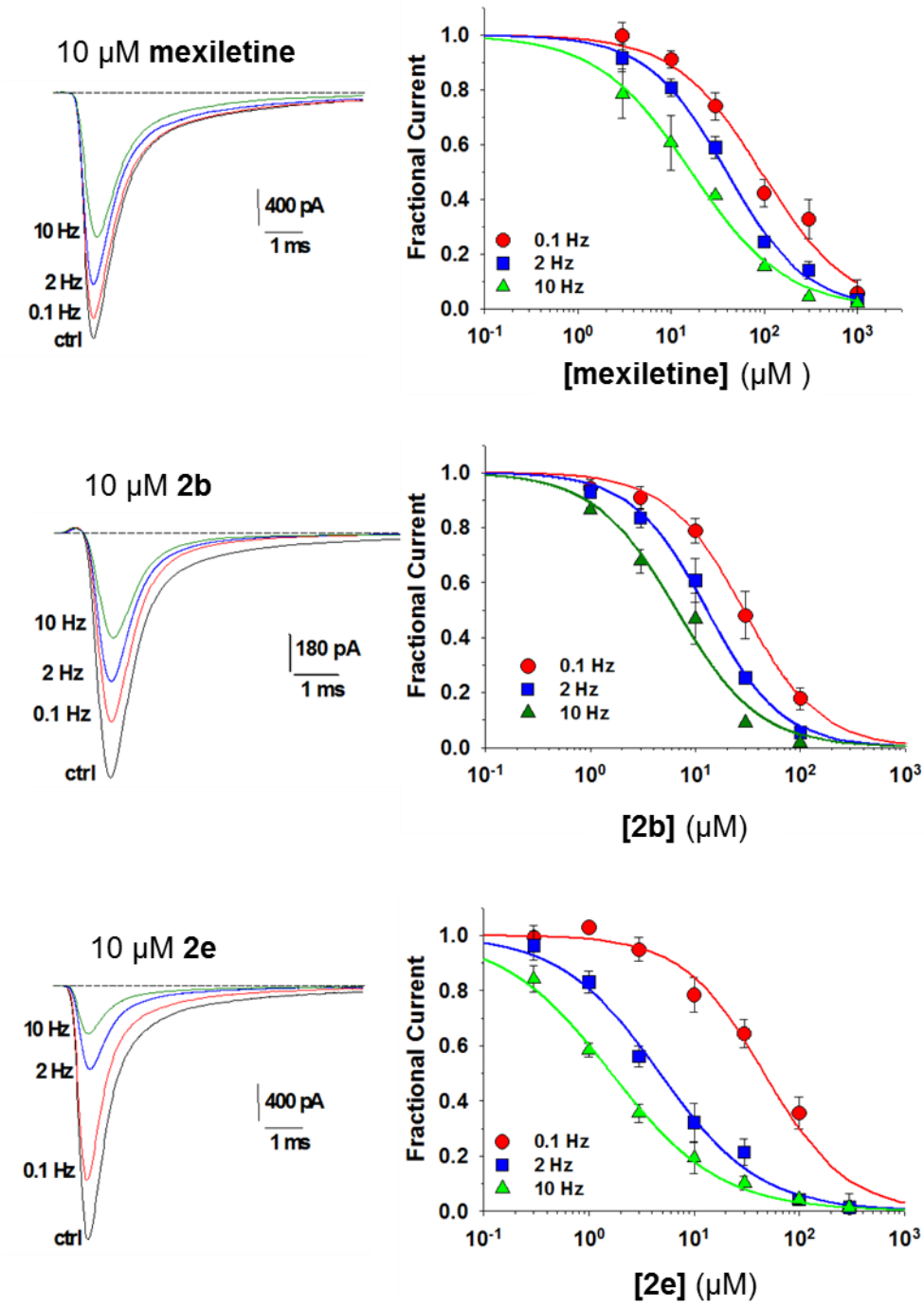

Figure 4:
Effects of mexiletine, **2b**, and **2e** on hNav1.5 channels: left column shows representative sodium current traces elicited from a holding potential of −120 mV to a test potential of −30 mV in the absence of drug (ctrl) and in the presence of 10 µM drug at 0.1, 2 or 10 Hz frequency stimulation. right column reports the corresponding concentration−response relationships fitted with a first–order binding equation described in material and methods. Each point is the mean ± SEM from 3-8 cells.

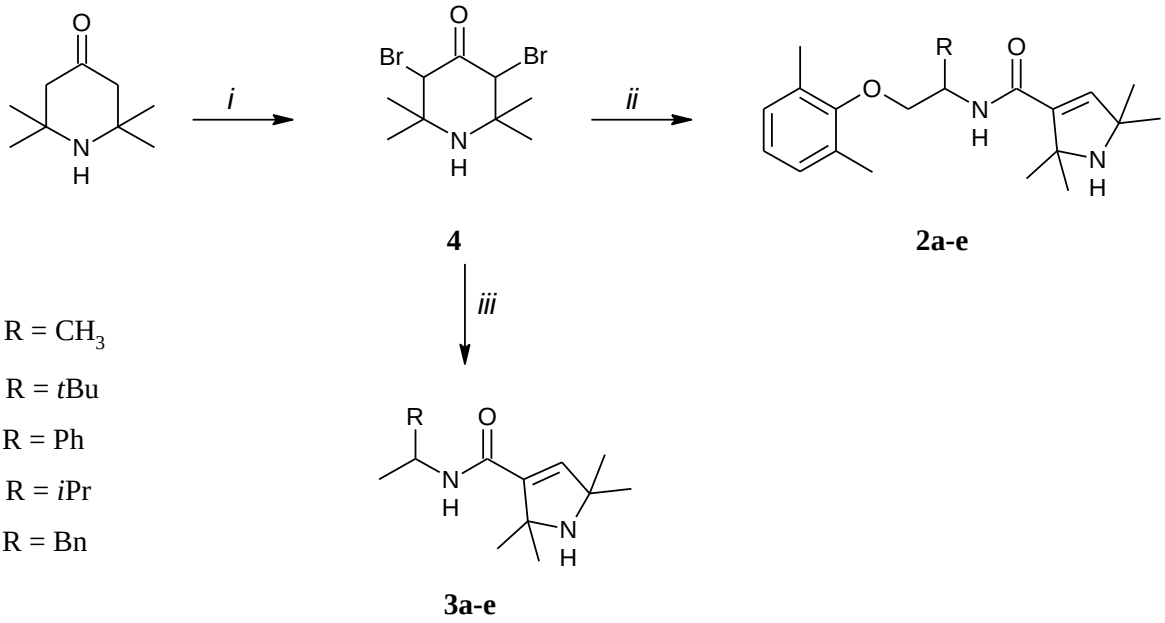

a: R = CH_3

b: R = *t*Bu

c: R = Ph

d: R = *i*Pr

e: R = Bn

Scheme 1. Reagents and conditions: (i) Br_2, AcOH, 60 °C; (ii) **1a–e**, TEA, H_2O, 50 °C; (iii) $NH_2CH(CH_3)R$, TEA, H_2O, 50 °C

Table 1. Anti-arrhythmic activity of compounds **2a–e**, **3a–e, mexiletine 1a** and its analogues **1b–e**

Compd	Max % increase[a] (mean ± SEM)	EC_{50}[b] (μM)	95% confidence limit (x 10^{-6})
2a	90 ± 2.9[c]	5.73	4.57–7.19
3a	46 ± 2.9[c]		
2b	144 ± 4.3[d]	0.054	0.024–0.12
3b	48 ± 1.3[e]		
2c	281 ± 9.1	4.04	3.05–5.83
3c	16 ± 0.7		
2d	76 ± 1.4[c]	1.33	1.01–1.74
3d	25 ± 1.6		
2e	74 ± 1.9[f]	0.41	0.37–0.83
3e	142 ± 6.5	8.07	6.38–8.94
mexiletine, 1a	64 ± 1.4[g]	11.61	8.71–13.47
1b	71 ± 2.4[c]	2.11	1.38–3.20
1c	135 ± 2.2[f]	0.43	0.34–0.54
1d	145 ± 4[g]	18.4	14.9–22.7
1e	169 ± 4[c]	4.36	1.47–6.38

[a]Increase of threshold of ac-arrhythmia: increase in the current strength of 50 Hz alternating current required to produce arrhythmia in guinea pig left atria driven at 1 Hz in the presence of each tested compounds at $5x10^{-5}$ M. For all data $P < 0.05$. [b]Calculated from log concentration-response curves (Probit analysis according to Litchfield and Wilcoxon[39] with n = 6–8). When the maximum effect was < 50%, the EC_{50} values were not calculated. [c]At 10^{-5} M. [d]At 10^{-6} M. [e]At 5 $x10^{-7}$ M. [f]At 5 x 10^{-6} M. [g]At 10^{-4} M.

Table 2. Conformational analysis on **2a–e** in vacuum.

Compd	no. of conformers[a]	Boltzmann weights	
		s-trans	***s-cis***
2a	4	1.00	0.00
2b	6	0.86	0.14
2c	6	1.00	0.00
2d	17	0.98	0.02
2e	18	0.96	0.04

[a]True conformers found in a 5 Kcal/mol window above the global minimum conformer energy

Table 3. Influence of tested compounds on cardiovascular parameters.

	Left atrium			Right atrium					
	negative inotropy			negative inotropy			negative chronotropy		
Compd	**Activity[a] (M ± S.E.M.)**	**EC_{50}[b] (μM)**	**95% conf lim ($x10^{-6}$)**	**Activity[c] (M ± S.E.M.)**	**EC_{50}[b] (μM)**	**95% conf lim ($x10^{-6}$)**	**Activity[d] (M ± S.E.M.)**	**EC_{50}[b] (μM)**	**95% conf lim ($x10^{-6}$)**
2a	90 ± 1.2	0.034	0.022–0.058	79 ± 3.2[i]	1.48	0.93–2.07	31 ± 2.4[i]		
3a	55 ± 1.9[e]	0.0073	0.0045–0.011	80 ± 1.8	0.075	0.051–0.10	5 ± 0.1		
2b	92 ± 1.6	0.18	0.13–0.21				54 ± 1.7[i]	1.54	1.11–2.13
3b	68 ± 2.4[e]	0.0019	0.0012–0.029	76 ± 1.5	0.080	0.056–0.11	5 ± 0.2[j]		
2c	97 ± 0.8[f]	0.12	0.079–0.17				62 ± 2.1[h]	3.64	3.04–4.35
3c	78 ± 2.9[e]	0.028	0.022–0.036	72 ± 3.7[h]	0.049	0.040–0.060	10 ± 0.6		
2d	95 ± 1.3[g]	0.012	0.0074–0.022	75 ± 1.9[g]	0.22	0.16–0.30	6 ± 0.3[g]		
3d	80 ± 2.5	0.038	0.024–0.062	62 ± 2.4[j]	0.063	0.049–0.082	8 ± 0.5[j]		
2e	95 ± 1.3[h]	1.25	0.98–1.59	89 ± 2.3[g]	0.057	0.041–0.082	44 ± 1.2[g]		
3e	87 ± 3.5	0.11	0.079–0.14	88 ± 2.4	0.65	0.40–0.98	19 ± 0.7		
mexiletine	90 ± 1.3	0.045	0.035–0.058				85 ± 2.6[k]	0.028	0.023–0.035

[a]Decrease in developed tension on isolated guinea-pig left atrium at 10^{-5} M, expressed as percent changes from the control (n = 5-6). The left atria were driven at 1 Hz. The 10^{-5} M concentration gave the maximum effect for most compounds. [b]Calculated from log concentration-response curves (Probit analysis by Litchfield and Wilcoxon[39] with n = 6-7). When the maximum effect was < 50%, the EC_{50} inotropic and EC_{50} chronotropic values were not calculated. [c]Decrease in developed tension on guinea-pig spontaneously beating isolated right atrium at $5x10^{-5}$ M, expressed as percent changes from the control (n = 7-8). The $5x10^{-5}$ concentration gave the maximum effect for most compounds. [d]Decrease in atrial rate on guinea-pig spontaneously beating isolated right atrium at $5x10^{-5}$ M, expressed as percent changes from the control (n = 7-8). The $5x10^{-5}$ M concentration gave the maximum effect for most compounds. Pretreatment heart rate ranged from 165 to 190 beats/min. [e]At the $5x10^{-7}$ M. [f]At the $5x10^{-5}$ M. [g]At the 10^{-6} M. [h]At the $5x10^{-6}$ M. [i]At 10^{-5} M. [j]At 10^{-4} M. [k]At the 10^{-7}

Table 4. Relaxant activity of compounds **2a–e**, **3a–e, mexiletine** on K^+-depolarized guinea pig vascular and non-vascular smooth muscle.

Cmpd	Aorta Activity[a] (M ± S.E.M.)	Activity[a] (M ± S.E.M.)	Ileum IC_{50}[b] (μM)	95% conf lim ($x10^{-6}$)
2a	10 ± 0.2	97 ± 0.1	12.22	9.23–15.32
3a	0.4 ± 0.01	27 ± 1.3		
2b	19 ± 0.6[c]	74 ± 1.2[d]	3.93	3.02–5.04
3b	3 ± 0.2[c]	41 ± 1.8		
2c	29 ± 2.2	96 ± 1.1[d]	4.16	3.27–4.98
3c	2 ± 0.1	39 ± 2.4		
2d	18 ± 0.2	96 ± 2.3	9.67	2.48–15.07
3d	0.2 ± 0.01	28 ± 1.8		
2e	30 ± 2.7[c]	60 ± 1.9[d]	2.22	1.03–3.48
3e	9 ± 0.7	33 ± 2.2		
mexiletine	5 ± 0.3	81 ± 1.9	8.52	6.54–11.09

[a]Percent inhibition of calcium-induced contraction on K^+-depolarized (80 mM) guinea pig aortic strips and longitudinal smooth muscle at 10^{-4} M. The 10^{-4} M concentration gave the maximum effect for most compounds. [b]Calculated from log concentration-response curves (Probit analysis by Litchfield and Wilcoxon[39] with n = 6–7). When the maximum effect was < 50%, the IC_{50} values were not calculated. [c]At the $5x10^{-5}$ M. [d]At the 10^{-5} M.

Table 5. Half-maximal concentrations and slope factors for tonic block (0.1 Hz) and use-dependent block (2 or 10 Hz) of hNav1.5 sodium currents by mexiletine, **2b**, and **2e** compounds. Fit parameter values are given with standard error of the fit.

Cmpd	frequency (Hz)	nH	IC_{50} (μM)	IC_{50} ratio
2b	0.1	1.2 ± 0.1	28 ± 2	
	2	1.2 ± 0.1	13 ± 1	2.2
	10	1.1 ± 0.2	6.6 ± 1.1	4.2
2e	0.1	1.1 ± 0.2	47 ± 7	
	2	0.9 ± 0.1	4.8 ± 0.5	9.8
	10	0.8 ± 0.1	1.6 ± 0.1	29.4
mexiletine	0.1	1.0 ± 0.1	93 ± 14	
	2	1.0 ± 0.1	40 ± 3	2.3
	10	0.9 ± 0.1	17 ± 2	5.5

Table 6. Physicochemical descriptors of compounds under study

Compd	pK_a[a]	Log P[a]	Log $D_{7.4}$[a]
2a	9.0 ± 0.7	5.0 ± 0.5	3.4
3a	9.0 ± 0.7	2.7 ± 0.4	1.1
2b	9.0 ± 0.7	6.2 ± 0.5	4.6
3b	9.0 ± 0.7	3.0 ± 0.4	1.4
2c	8.9 ± 0.7	6.3 ± 0.6	4.8
3c	9.0 ± 0.7	4.0 ± 0.5	2.5
2d	9.0 ± 0.7	5.8 ± 0.5	4.3
3d	9.0 ± 0.7	2.7 ± 0.4	1.1
2e	9.0 ± 0.7	6.6 ± 0.6	5.1
3e	9.0 ± 0.7	4.2 ± 0.5	2.6
mexiletine, 1a	8.58 ± 0.10	2.16 ± 0.23	1.0
1b	8.76 ± 0.17	3.39 ± 0.24	2.0
1c	8.48 ± 0.29	3.34 ± 0.29	2.2
1d	8.70 ± 0.13	3.04 ± 0.23	1.7
1e	7.84 ± 0.10	3.86 ± 0.24	3.3

[a]ACDlabs 7.09, Toronto, Canada.

Table 7. Antioxidant potencies in the DCFH-DA assay for mexiletine and the set of compounds under study.

Cmpd	DCFH-DA[a] IC_{50} ± SEM (μM)
2a	149 ± 2
3a	> 300
2b	157 ± 1
3b	> 300
2c	158 ± 8
3c	305 ± 14
2d	160 ± 2
3d	> 300
2e	150 ± 4
3e	> 300
mexiletine	202 ± 9

[a]Values are the mean of at least three determinations performed in sextuplicate.

References

[1] A. J. Kattoor, N. V. K. Pothineni, D. Palagiri, J. L. Mehta, *Curr. Atheroscler. Rep.* **2017**, *19*(11), article number 4.
[2] Q. C. Meng, *Curr. Top. Med. Chem.* **2006**, *6* (2), 93–102.
[3] D. J. Lefer, D. N. Granger, *Am. J. Med.* **2000**, *109*(4), 315–323.
[4] Z. Liu, T. Zhou, A. C. Ziegler, P. Dimitrion, L. Zuo, *Oxid. Med. Cell. Longev.* **2017**.
[5] W. J. Huang, X. I. A. Zhang, W. W. Chen, *Biomed. Rep.* **2016**, *4*(5), 519–522.
[6] B. J. Tabner, S. Turnbull, O. El-Agnaf, D. Allsop, *Curr. Top. Med. Chem.* **2001**, *1* (6), 507–517.
[7] T. Jiang, Q. Sun, S. Chen, *Prog. Neurobiol.* **2016**, *147*, 1–19.
[8] V. Triggiani, F. Resta, E. Guastamacchia, C. Sabbà, B. Licchelli, S. Ghiyasaldin, E. Tafaro, *Endocr. Metab. Immune Disord. Drug Targets* **2006**, *6*, 77–93.
[9] M. H. Choi, J. R. Ow, N. D. Yang, R. Taneja, *Oxid. Med. Cell. Longev.* **2016**, volume *2016*, Article ID 6842568
[10] L. C. P. Azevedo, M. Janiszewski, F. G. Soriano, F. R. M. Laurindo, *Endocr. Metab. Immune Disord. Drug Targets* **2006**, *6* (2), 159–164.
[11] E. Demirpençe, H. Caner, M. Bavbek, K. Kilinç, *Jpn. J. Pharmacol.* **1999**, *81*, 7–11.
[12] O. Ates, S. R. Cayli, E. Altinoz, N. Yucel, A. Kocak, O. Tarim, A. Durak, Y. Turkoz, S. Yologlu, *Mol. Cell. Biochem.* **2006**, *286* (1), 125–131.
[13] C. Z. Chang, D. Winardi, J. K. Loh, S. S. Kung, S. L. Howng, A. Y. Jeng, A. -L. Kwan, *Acta Neurochir.* **2002**, *144*, 189–193
[14] H. Li, K. Y. Xu, L. Zhou, T. Kalai, J. L. Zweier, K. Hideg, P. Kuppusamy, *J. Pharmacol. Exp. Ther.* **2000**, *295*, 563–571.
[15] A. Toth, R. Halmosi, K. Kovacs, P. Deres, T. Kálai, K. Hideg, K. Toth, B. Sumegi, *Free radic. Boil. Med.* **2003**, *35*, 1051–1063.
[16] M. De Bellis, A. De Luca, J.-F. Desaphy, R. Carbonara, J.A. Heiny, A. Kennedy, A. Carocci, M.M. Cavalluzzi, G. Lentini, C. Franchini, D. Conte Camerino, *Biophys. J.* **2013**, *104*, 344–354.
[17] A. Carocci, A. Catalano, A. Bruno, G. Lentini, C. Franchini, M. De Bellis, A. De Luca, D. Conte Camerino, Synthesis and in vitro sodium channel blocking activity evaluation of novel homochiral mexiletine analogs. *Chirality* **2010**, *22*, 299−307.
[18] M. Roselli, A. Carocci, R. Budriesi, M. Micucci, M. Toma, L. Di Cesare Mannelli, A. Lovece, A. Catalano, M.M. Cavalluzzi, A. De Palma, M. Contino, M. G. Perrone, N. A. Colabufo, C. Franchini, C. Ghelardini, S. Habtemariam, G. Lentini, *Eur. J. Med. Chem.* **2016**, *121*, 300–307.
[19] M. De Bellis, F. Sanarica, A. Carocci, G. Lentini, S. Pierno, J. F. Rolland, D. Conte Camerino, A. De Luca, *Front. Pharmacol.* **2018**, *8*, 907.
[20] S. W. Stork, M. W. Makinen, *Synthesis* **1999**, *8*, 1309–1312
[21] M. Groesbeek, J. Lugtenburg, *Recueil des Travaux Chimiques des Pays-Bas* **2010**, *114*, 403–409.
[22] O. H. Hankovsky, K. Hideg, I. Bodi, L. Frank, *J. Med. Chem.* **1986**, *29* (7), 1138–1152.
[23] A. De Luca, S. Talon, M. De Bellis, M., J. -F.Desaphy, C. Franchini, G. Lentini, G., et al. *Naunyn Schmiedebergs Arch. Pharmacol.* **2003**, *367*, 318–327.
[24] A. Duranti, C. Franchini, G. Lentini, F. Loiodice, V. Tortorella, A. De Luca, S. Pierno, D. Conte Camerino, *Eur. J. Med. Chem.* **2000**, *35* (1), 147–156.
[25] G. Lentini, G. Milani, S. Habtemariam, *ACS Sustainable Chem. Eng.* **2019**, *7* (7), 6424–6425.
[26] R. Gualdani, F. Tadini-Buoninsegni, M. Roselli, I. Defrenza, M. Contino, N. A. Colabufo, G. Lentini, *Pharmacol. Res. Perspect.* **2015**, *3* (5), e00160.
[27] M. L. Verdonk, D. C. Rees, *ChemMedChem* **2008**, *3*, 1179–1180
[28] R. Gualdani, M. M. Cavalluzzi, F. Tadini-Buoninsegni, M. Convertino, P. Gailly, A. Stary-Weinzinger, G. Lentini, *Cell. Physiol. Biochem.* **2018**, *45* (6), 2233–2245.

[29] A. Catalano, J. -F. Desaphy, G. Lentini, A. Carocci, A. Di Mola, C. Bruno, R. Carbonara, A. De Palma, R. Budriesi, C. Ghelardini, M. G. Perrone, N. A. Colabufo, D. Conte Camerino, C. Franchini, *J. Med. Chem.* **2012**, *55*(3), 1418–1422.
[30] J. -F. Desaphy, R. Carbonara, T. Costanza, D. Conte Camerino, *Exp. Neurol.* **2014**, *255*, 96–102.
[31] C. Franchini, A. Carocci, A. Catalano, M. M. Cavalluzzi, F. Corbo, G. Lentini, A. Scilimati, P. Tortorella, D. Conte Camerino, A. De Luca, *J. Med. Chem.* **2003**, *46*, 5238−5248.
[32] A. Carocci, A. Catalano, C. Bruno, G. Lentini, C. Franchini, M. De Bellis, A. De Luca, D. Conte Camerino, *Chirality* **2010**, 22, 299−307.
[33] M. M. Cavalluzzi, P. Imbrici, R. Gualdani, A. Stefanachi, G. F. Mangiatordi, G. Lentini, O. Nicolotti, *Drug Discov. Today* **2020**, *25* (2), 344–366.
[34] F. Lovering, J. Bikker, C. Humblet, *J. Med. Chem.* **2009**, *52* (21), 6752–6756.
[35] M. M. Cavalluzzi, G. F. Mangiatordi, O. Nicolotti, G. Lentini, *Exp. Opin. on Drug Discov.* **2017**, *12* (11), 1087–1104.
[36] A. Catalano, R. Budriesi, C. Bruno, A. Di Mola, I. Defrenza, M. M. Cavalluzzi, M. Micucci, A. Carocci, C. Franchini, G.Lentini, G. *Eur. J. Med. Chem.* **2013**, *65*, 511–516.
[37] W. C. Still, M. Kahn, A. Mitra, *J. Org. Chem.* **1978**, *43*, 2923–2925.
[38] B. Tasso, R. Budriesi, I. Vazzana, P. Ioan, M. Micucci, F. Novelli, M. Tonelli, A. Sparatore, A. Chiarini, F. Sparatore, *J. Med. Chem.* **2010**, *53*(12), 4668–4677.
[39] R. J. Tallarida, R. B. Murray, *Manual of Pharmacologic Calculations with Computer Programs*, 2nd ed.; Springer-Verlag: New York, **1987**.
[40] H. Motulsky, A. Christopoulos, Fitting Models to Biological Data Using Linear and Non Linear Regression. **2003**, *www.graphpad.com*.
[41] H. J. Motulsky, Prism 5 Statistics Guide; GraphPad Software Inc.: San Diego, CA, **2007**; www.graphpad.com.
[42] J. -F. Desaphy, A. Dipalma, M. De Bellis, T. Costanza, C. Gaudioso, P. Delmas, A. L. George, D. Conte Camerino, *PAIN*® **2009**, *142*(3), 225–235.
[43] H. Wang, J. A. Joseph, *Free Radic. Biol. Med.* **1999**, *27*, 612–616.
[44] T. A. Halgren, *J. Comput. Chem.* **1996**, *17*, 490–519.
[45] A. D. Becke, *Phys. Rev. A* **1988**, *38*, 3098–3100.
[46] E. R. Davidson, D. Feller, *Chem. Rev.* **1986**, *86*, 681–696.